Published in final edited form as:
Circulation. 2011 December 20; 124(25): 2812–2821. doi:10.1161/CIRCULATIONAHA.111.056309.

Mice with cardiac overexpression of PPARγ have impaired repolarization and spontaneous fatal ventricular arrhythmias (Morrow, PPARγ overexpression induces fatal arrhythmias)

John P. Morrow, MD[1,*], **Alexander Katchman, PhD**[1], **Ni-Huiping Son, MD**[2], **Chad M. Trent, BS**[2], **Raffay Khan, MD**[2], **Takayuki Shiomi, MD**[3], **Haiyan Huang, MD, PhD**, **Vaibhav Amin, BS**[1], **Joshua M. Lader, MD**[5], **Carolina Vasquez, PhD**[5], **Gregory E. Morley, PhD**[5], **Jeanine D'Armiento, MD, PhD**[3], **Shunichi Homma, MD**[1], **Ira J. Goldberg, MD**[2], and **Steven O. Marx, MD**[1,4]

[1]Division of Cardiology, College of Physicians and Surgeons of Columbia University; New York, NY 10032

[2]Preventive Medicine, College of Physicians and Surgeons of Columbia University; New York, NY 10032

[3]Molecular Medicine, College of Physicians and Surgeons of Columbia University; New York, NY 10032

[4]Department of Medicine, and Department of Pharmacology, College of Physicians and Surgeons of Columbia University; New York, NY 10032

[5]Division of Cardiology, NYU School of Medicine

Abstract

Background—Diabetes and obesity, which confer an increased risk of sudden cardiac death, are associated with cardiomyocyte lipid accumulation and altered cardiac electrical properties, manifested by prolongation of the QRS duration and QT interval. It is difficult to distinguish the contribution of cardiomyocyte lipid accumulation versus the contribution of global metabolic defects to the increased incidence of sudden death and electrical abnormalities.

Methods and Results—In order to study the effects of metabolic abnormalities on arrhythmias without the complex systemic effects of diabetes and obesity, we studied cardiac-specific transgenic mice expressing PPARγ1 via the cardiac α-myosin heavy-chain promoter. The PPARγ-transgenic mice develop abnormal accumulation of intracellular lipids and die as young adults, prior to a significant reduction in systolic function. Using implantable ECG telemeters, we found that these mice have prolongation of the QRS and QT intervals, and spontaneous ventricular arrhythmias, including polymorphic ventricular tachycardia and ventricular fibrillation. Isolated cardiomyocytes demonstrated prolonged action potential duration caused by reduced expression and function of the potassium channels responsible for repolarization. Short-term exposure to

[*]Address correspondence to: John Morrow Columbia University, Division of Cardiology PH 10-203, 622 W.168th Street New York, NY 10032 Tel:(212)305-5553 Fax:(212)305-4648 jpm46@columbia.edu.

Subjects: Arrhythmias, Energy metabolism, Animal models of human disease, Ion channels

Disclosures: none

pioglitazone, a PPARγ agonist, had no effect on mortality or rhythm in WT mice, but further exacerbated the arrhythmic phenotype and increased the mortality in the PPARγ TG mice.

Conclusions—Our findings support an important link between PPARγ activation, cardiomyocyte lipid accumulation, ion channel remodeling and increased cardiac mortality.

Keywords

arrhythmia; metabolism; ion channels

Introduction

Diseases that affect cardiac energy metabolism and increase cardiomyocyte lipid stores, such as diabetes and obesity, are frequently associated with altered mechanical and electrical function in the heart, a syndrome termed lipotoxic cardiomyopathy [1-3]. After adjusting for other cardiovascular risk factors, both diabetes and obesity confer an increased risk of sudden cardiac death [4-8], and are associated with altered cardiomyocyte electrical properties, manifested by prolongation of the QRS and QT intervals [9-11]. The molecular mechanisms responsible for alterations in the electrical properties of cardiomyocytes and the increased incidence of sudden cardiac death have not been well elucidated. An essential question is whether the diabetes-induced cardiomyocyte lipid accumulation or the diabetes-induced global metabolic defects cause the increased incidence of sudden death.

In contrast to diabetic patients, several models of cardiac lipid accumulation have not shown increased mortality. Transgenic (TG) mice with cardiac-restricted over-expression of the peroxisome proliferation-activated receptor α (PPARα) exhibit a cardiac metabolic phenotype that is similar to that of the diabetic heart: increased fatty acid utilization and decreased uptake and oxidation of glucose [12]. These mice, which develop cardiomyocyte lipid accumulation, demonstrate reduced potassium (K^+) channel repolarizing currents. In contrast to diabetic patients, however, TG-PPARα mice do not have significant prolongation of the cardiac action potential duration (APD) and do not have increased incidence of sudden death [13]. Mice with cardiac-restricted over-expression of the fatty-acid transport protein 1 (FATP1), which develop cardiomyocyte lipid accumulation, demonstrate prolongation of the QT_c interval due to a reduction in repolarizing voltage-gated K^+ currents [14]. These mice only have increased mortality when pregnant.

PPARγ, a transcription factor that causes lipid accumulation, insulin sensitivity and reduced inflammation in the vessel wall [15, 16], is typically expressed at relatively low levels in the heart. PPARγ suppresses cardiac growth and embryonic gene expression [17]. PPARγ is expressed at higher levels in the human heart, especially in humans with metabolic syndrome, than in the murine heart [18, 19]. PPARγ is activated by rosiglitazone and pioglitozone, drugs that are associated with heart failure and, in the case of rosiglitazone, greater cardiac mortality [20]. Mice with cardiac-restricted overexpression of PPARγ have abnormal accumulation of intracellular lipids in cardiomyocytes, gradually develop a dilated cardiomyopathy and die suddenly in young adulthood, often prior to a reduction in systolic function; this premature demise is exacerbated by treatment with rosiglitazone [18]. We found that these mice have spontaneous ventricular tachyarrhythmias causing sudden death, secondary to electrical remodeling. Although short-term exposure to pioglitazone, a more commonly used PPARγ agonist, had no effect on mortality and spontaneous ventricular arrhythmias in WT mice, pioglitazone further exacerbated the arrhythmic phenotype and increased the mortality in the TG-PPARγ mice. Our findings support an important link between cardiac PPARγ activation, cardiomyocyte lipid accumulation and the cardiac

electrophysiological remodeling, and describe a model for the greater incidence of sudden death in patients with diabetes.

Methods

A detailed description of methods and reagents used is provided in the online Supplement.

Telemetry, ECG analysis and Monophasic Action Potential (MAP) Recordings

Telemetry devices (Data Sciences International, model EA-F20) were implanted in 10 week-old mice. Recordings were begun 1 week after implantation. Intervals were measured manually using Ponemah 3 software. For *in vivo* MAP recordings, under general anesthesia, a thoracotomy was made between the ribs of the left side of the thorax, and a 0.25 mm-tip electrode was pressed lightly against the anterior surface of the left ventricle (LV). The ground electrode was pressed against the inner surface of the rib cage. Signals were amplified and filtered as described[21].

Echocardiography

Transthoracic echocardiography was performed on isoflurane-anesthetized mice using a high-resolution imaging system with a 30-MHz imaging transducer (Vevo 770; VisualSonics) [18].

Isolation of Cardiomyocytes and Cellular Electrophysiology

Cardiomyocytes were isolated using methods previously described [22]. Membrane currents, of non-contracting rod-shaped cells with clear striations, were measured by the whole-cell patch-clamp method [23] using a MultiClamp 700B amplifier (Axon Instruments, Union City, CA). Solutions and voltage clamp methodologies are further described in the supplement.

Optical mapping

High-resolution optimal mapping experiments were performed on 16-week old TG-PPARγ and WT littermate control mice as previously described [24-26]. Briefly, hearts were isolated and perfused by the Langendorff method with warm (37°C) oxygenated Tyrode's solution. After stabilization, the heart was stained with the voltage-sensitive dye Di-4-ANEPPs (8μL of 2-mmol/L stock solution dissolved in DMSO), and contraction was inhibited with blebbistatin (5μM). The heart was stimulated with a platinum electrode at 100 ms intervals.

Real-time PCR

Samples of ventricular tissue from 10-12 week old PPARγ and WT littermate mice were used for RT-PCR. Real-time PCR was performed using an Applied Biosystems StepOne Plus Real-Time PCR system and inventoried primers (Applied Biosystems). PCR reactions were performed, in duplicate, for 40 cycles with automated detection of crossing threshold.

Immunoblots

The preparation and immunoblotting of heart homogenates was performed as described [27]. Chemiluminescence signal was obtained using a Kodak Image Station and signal intensities quantified using ImageJ software.

Immunohistochemistry

Heart tissue was fixed with 4% paraformaldehyde, embedded in paraffin wax, and then sectioned. Sections were incubated with anti-Cx43 (1:200) or non-immune rabbit polyclonal IgG at 4°C overnight. For DAB staining, sections were exposed sequentially to 0.3% H_2O_2,

anti-rabbit swine antibody conjugated to biotin (1:500, DakoCytomation) for 1 hr, peroxidase-labeled ABC (VECTASTAIN ABC Kit, Vector Laboratories), and finally developed with DAB solution (ImmPACT DAB Peroxidase Substrate, Vector Laboratories). Sections were counterstained with hematoxylin. For immunofluorescent staining, after reaction with anti-rabbit donkey antibody conjugated to Alexa Fluor 488 (1:500, Invitrogen), sections were counterstained with DAPI.

Statistical Analysis

Results are presented as mean ±SEM. The nonparametric Mann–Whitney U-test was used for comparisons with n<10, and the unpaired *t*-test with equal variances was used for comparisons of larger groups. A 2-tailed value of $P<0.05$ was considered statistically significant, except for ECG intervals and PVC burden where the Bonferroni correction was used for multiple comparisons. Linear regression analysis was performed using GraphPad Software.

Results

Two lines of TG-PPARγ1 mice have been developed and reported[18], showing similar phenotypes, albeit with different severities. The high-expressing line (MHC-PPARγ1H) demonstrated a reduced ejection fraction by 4 months of age. The MHC-PPARγ1H mice had significantly reduced lifespan, with 50% mortality at 3 months of age, prior to the clinical development of heart failure[18]. The MHC-PPARγ1H mouse line was used for all experiments.

Young adult PPARγ mice have normal echocardiograms and histology

We performed echocardiography of 10-12 week old MHC-PPARγ and WT littermate mice. LV systolic dimension and fractional shortening were within normal limits[28] for PPARγ mice at this age (Figure 1A-C). Histological examination did not demonstrate increased fibrosis (Figure 1D). These results suggest that the increased mortality is not related to systolic dysfunction or fibrosis. Gross structural analysis revealed that the thickness and fiber direction across the ventricular walls did not change significantly in the 10-12 week old PPARγ mice compared WT littermate controls (Figure 1D). The PPARγ mice have mild cardiac hypertrophy, since the heart-weight:body-weight ratio is modestly increased, 13% above WT (Supplemental Figure 1), consistent with prior reports from PPARγ–agonist treated mice[17].

PPARγ mice have fatal ventricular arrhythmias

We hypothesized that an arrhythmia was the most likely cause of the sudden death, and implanted telemeters to monitor the heart rhythm of 10 week-old MHC-PPARγ and WT littermate mice. Echocardiograms, performed prior to telemeter-implantation, demonstrated normal LV size and function. The average daily heart rate of the TG-PPARγ mice was similar to WT mice at 12 and 16 weeks of age (Figure 2A). The QRS duration was significantly prolonged for 16 week-old TG-PPARγ mice compared to age-matched WT littermates (Figure 2B, 2C). The QT interval was significantly prolonged at 12 and 16 weeks in TG-PPARγ mice compared with WT (Figure 2B, 2D).

The TG-PPARγ mice had significantly increased ventricular arrhythmias compared to WT at 12 and 16 weeks of age. Premature ventricular complexes (PVCs) were frequent in the PPARγ mice, averaging 7.4 PVCs/hour in 12 week-old mice, compared to less than 0.2 PVCs/hour (approximately 5 PVCs/day) in age-matched WT mice (Figure 2E). Complex ectopy, such as paired PVCs or non-sustained VT, occurred frequently in TG-PPARγ mice (0.08/hour at 12 weeks, 1.2/hour at 16 weeks), and was never observed in WT littermates.

Sustained VT was the cause of death in two of three TG-PPARγ mice undergoing long-term-monitoring; the third mouse died from bradycardia. Death due to bradycardia is common in TG mouse models of heart disease, whereas death from spontaneous VT is unusual[29, 30].

Prolonged action potential duration (APD) and decreased K^+ current density in PPARγ mice

The prolongation of the QT interval may be due to abnormalities in cardiomyocyte depolarization and/or repolarization. Monophasic action potentials (MAP), which are extracellular waveforms, were used to quantify ventricular repolarization. We measured the MAP in WT and TG-PPARγ mice through a small thoracotomy, by placing an electrode on the anterolateral surface of the beating heart during normal sinus rhythm. The APD measurements in WT mice are similar to the *in vitro* findings previously reported for murine heart [21]. We found that the APD_{20} (PPARγ: 5.2 ± 0.7 ms; WT 2.4 ± 0.3 ms; $p<0.01$) and APD_{50} (PPARγ: 10.7 ± 1.0 ms; WT 5.9 ± 0.4 ms; $p<0.01$) were significantly prolonged in 12-week-old TG-PPARγ mice compared to age-matched littermates (Figure 3A, 3B). The APD_{90} was not significantly different in TG-PPARγ and WT mice, $p=0.44$. In the TG-PPARγ mice, the longer phase 2 of the action potential likely causes increased activation of K^+ currents in phase 3 of the action potential, enabling a compensatory faster phase-3 repolarization. The prolongation of early repolarization (APD_{20} and APD_{50}), without significant prolongation of the APD_{90}, can be arrhythmogenic[31].

The action potential waveforms, measured using the perforated patch clamp technique at 35°C and stimulating at 1000ms intervals, were prolonged in the ventricular myocytes from 10-12 week-old TG-PPARγ mice compared to age-matched WT littermate controls (Figure 3C). Consistent with the *in vivo* MAP recordings, the APD_{20} and APD_{50} in the TG-PPARγ cardiomyocytes were significantly increased compared to control cardiomyocytes ($p<0.001$; Figure 3D). The APD_{90} in the TG-PPARγ cardiomyocytes was also significantly increased compared to control cardiomyocytes ($p<0.001$; Figure 3B). The difference in rate between the MAP recordings and patch-clamp recording may explain the difference in APD_{90} estimates, since rate can modify repolarization currents and calcium handling.

The repolarization phase of the cardiac action potential is dependent upon a balance between inward depolarizing Ca^{2+} and Na^+ currents, and outward repolarizing K^+ currents. Whole-cell currents were recorded at room temperature from 10-12 week-old TG-PPARγ mice and corresponding age-matched littermate controls. Voltage-dependent Na^+ and Ca^{2+} current densities and current-voltage (I-V) relationship were similar in the TG-PPARγ and WT mice (Figure 4A, 4B). Boltzmann fits of the activation and inactivation revealed no changes in Na^+ and Ca^{2+} channels' V_{50} for activation and for inactivation. A late, persistent Na^+ current was not observed in the TG-PPARγ mice (Figure 4A, insets). The voltage-dependent K^+ currents, in contrast, were significantly altered in the PPARγ mice compared to the WT mice (Figure 4C). In mice at least four distinct voltage-dependent K^+ currents have been identified [32, 33]. Peak outward K^+ current ($I_{K,peak}$) was reduced in the PPARγ mice (44.2 ± 4.2 pA/pF) compared to WT mice (60.4 ± 5 pA/pF; $p=0.02$). The decay phases of the voltage-dependent K^+ currents in adult mouse cardiomyocytes may be fit [13] by the sum of two exponentials, which denote the fast transient K^+ current, $I_{to,f}$, a rapidly activating, very slowly inactivating current, $I_{K,slow}$, and a non-inactivating current, I_{ss}[32, 33]. Analysis of the decay phases demonstrated a statistically significant reduction in the current density of $I_{K,\,slow}$ (WT: 23.8 ± 2.1 pA/pF; PPARγ : 14.1 ± 1.3 pA/pF; $p<0.001$), and a non-statistically significant reduction in current densities of $I_{to,f}$ (WT: 22.4 ± 2.8 pA/pF; PPARγ: 16.2 ± 3 pA/pF; $p=0.15$) (Figure 4C). There was no significant change in the current density of I_{ss} (WT: 10.8 ± 0.8 pA/pF; PPARγ: 11.8 ± 0.8 pA/pF; $p=0.34$) (Figure 4C, 4D) or the current density of the inward rectifying current, I_{K1} (not shown), in the TG-PPARγ mice compared

to WT mice. Cardiomyocytes had the same average size as shown by whole-cell membrane capacitance; the resting membrane potential and action potential amplitude (APA) were not significantly different in the PPARγ and WT littermate controls (see Supplement table 1.).

The reduction in the $I_{K,slow}$ current density in the TG-PPARγ mice was confirmed using a pharmacological approach. After exposure to 50 μmol/L 4-AP, WT cardiomyocytes showed a marked reduction in $I_{K,slow}$ (Figure 5A). The 4-AP-sensitive $I_{K,slow}$ current, however, was markedly reduced in cardiomyocytes from PPARγ mice (Figure 5A, 5B). Linear regression of the 4-AP-sensitive current demonstrated a significant difference in the slopes (pA/pF/mV) for the WT and PPARγ mice (WT: 0.211 ± 0.002; PPARγ: 0.126 ± 0.002; p=0.002; n=21 and 26, respectively). These data suggest that the prolongation of APD in PPARγ mice was primarily due to a reduction in $I_{K,slow}$ current. We also measured the effect of 4-AP inhibition on APD concurrently, by switching from voltage-clamp to current clamp mode. Intracellular calcium was buffered to 10 nM, at a temperature of 22°C to optimize cardiomyocyte condition. Under these conditions, the APD in PPARγ was still prolonged. Blocking 4-AP-sensitive current in WT cardiomyocytes prolonged the APD to a larger extent than in PPARγ cardiomyocytes. After exposure to 4-AP, the APD was not significantly different in WT and PPARγ mice (Figure 5C).

Reduced expression of voltage-dependent K^+ channels in PPARγ hearts

Gene expression was determined by real-time quantitative PCR of RNA extracted from the ventricular tissue of 10-12 week mice. The mRNA expression of $K_V2.1$, which contributes to $I_{K,slow}$[34, 35] was significantly reduced in the TG-PPARγ mice, as compared to WT littermates. The mRNA expression of $K_V4.2$, which encodes $I_{to,f}$[36] was not significantly reduced. In contrast to larger animals, $K_V4.3$ is not required for functional $I_{to,f}$ in the mouse [37]. Protein expression of the voltage-dependent K^+ channels was measured using ventricular homogenates. In contrast to the modest or absent changes in mRNA expression, the protein expression of these channels was markedly reduced in the TG-PPARγ mice (Figure 6B, 6C). The protein levels of $K_V1.5$ and $K_V2.1$, that form $I_{K,slow}$ in mouse, was significantly reduced to 67% and 50%, respectively, of WT littermate controls. These reductions in protein expression are consistent with the findings of reduced $I_{K,slow}$ current density (Figure 5). The protein expression of $K_V4.2$, which forms $I_{to,f}$, was also markedly reduced in the PPARγ mice, to 27% of the control level. Although the current density of $I_{to,f}$ was reduced in the PPARγ mice, the reduction in protein expression of this subunit is far greater, suggesting up-regulation of activity of the remaining $K_V4.2$. The $K_v1.4$ channel, which also contributes to I_{to}, is also reduced significantly.

Prolongation of APD does not cause triggered activity

To better understand the mechanisms of ectopy and arrhythmia, ventricular myocytes were paced through the patch pipette in perforated configuration by current pulses (amplitude 0.1 - 0.4 nA, 3 ms duration) at intervals from 1000 to 250 msec. Under these conditions, we did not observe any early after-depolarizations (EADs) or delayed after-depolarizations (DADs) in PPARγ or WT cardiomyocytes (n=32, from 3 mice in each group).

Connexin43 is reduced but conduction velocity is normal

Connexin43 (Cx43, the major ventricular gap junction protein) mRNA and protein expression was significantly downregulated in the PPARγ mice, to 31% (Figure 7A) and 14% (Figure 7B, 7C) respectively of WT littermates. Other intercalated disk proteins, such as cadherin and plakoglobin were also reduced (Figure 7C). Cx43 was decreased throughout the heart, as determined by immunohistochemistry of sections isolated from the anterior (Ant), lateral (Lat), and posterior (Post) walls of the LV, and the right ventricle (RV) (Figure 7D). The reduction in Cx43 occurred prior to the development of systolic dysfunction. To

assess the effect of Cx43 reduction on ventricular impulse propagation, we optically mapped cardiac activation patterns in the PPARγ and WT littermate mice. Surprisingly, the minimum conduction velocity (CV_{min}) was not significantly reduced in the PPARγ mice compared to the control littermate mice (p=0.55 for LV) (Figure 7F). Thus, it is not likely that the reduction in expression of Cx43 accounts for the increased propensity to develop ventricular arrhythmias and sudden death.

PPARγ agonist, pioglitazone, increases ventricular arrhythmias in TG-PPARγ mice

TG-PPARγ and WT littermates, 10-12 weeks of age, were fed standard mouse chow or pioglitazone-impregnated standard mouse chow for 3 weeks. Pioglitazone increased the mortality in the PPARγ mice (pioglitazone-chow: 75% vs. control-chow: 25%, n=8 in each group) during the 3-week period, but had no effect on mortality in the WT littermate animals (Figure 8A). To determine the mechanism(s) responsible for the pioglitazone-induced increased mortality in the TG-PPARγ mice, ECG telemeters were implanted into four 10-week-old TG-PPARγ mice and four WT littermate mice. Baseline telemetric measurements were initiated 4 days post-implantation. Mice were then fed pioglitazone for 7 days. For TG-PPARγ mice, within 4 days of starting pioglitazone, there was a significant increase in PVCs per hour; by day 6 of pioglitazone-chow the number of PVCs per hour was 15 times the baseline rate (p=0.0285 by U-test). Complex ventricular ectopy also increased approximately 15-fold over the same time period (Figure 8B, 8C). Linear regression modeling of the time course shows a slope that is significantly different from zero (F-test = 0.017). Complex ventricular arrhythmias were never observed in the WT littermate mice, in the absence or presence of pioglitazone ingestion, and even after 3 weeks of pioglitazone chow the WT mice did not have an increase in PVCs/hour. During the relatively short (and intermittent) monitoring period, sudden cardiac death was captured in one TG-PPARγ animal caused by spontaneous polymorphic ventricular tachycardia degenerating to ventricular fibrillation. We examined the ion channel protein expression from the hearts of TG-PPARγ mice fed either control-or pioglitazone-chow for 1 week. $K_V1.5$, which encodes I_{Kslow}, was decreased by 35% (Figure 8C) in the pioglitazone-fed TG-PPARγ mice compared to control-chow-fed TG-PPARγ mice (p=0.11 by U-test). These results suggest that PPARγ-agonist induced activation of PPARγ, when over-expressed in the heart, has a deleterious effect on mortality and arrhythmogenesis.

Discussion

Despite the increasing prevalence of obesity and diabetes, little is known about the contribution of metabolic abnormalities to the pathophysiology of arrhythmias and sudden cardiac death. Increased cardiomyocyte lipid stores are observed in obese and diabetic patients and this may contribute to arrhythmias. In diabetic patients, plasma free fatty acid concentration correlates with the frequency of ventricular premature complexes, and patients with ischemic cardiomyopathy and obesity have more VT than non-obese patients with ischemic cardiomyopathy [38, 39]. Diabetes and obesity are also associated with an increased risk of cardiomyopathy, independent of the presence of hypertension or coronary artery disease, which may represent a direct toxic effect of increased intracellular lipids [2, 40]. We used a gain-of-function approach to show that cardiomyocyte-specific metabolic derangements associated with the cardiac-specific overexpression of PPARγ leads to ventricular arrhythmias and sudden cardiac death. The over-expression of PPARγ, which can regulate transcription of numerous targets, and/or the subsequent cardiomyocyte lipid accumulation led to reductions in the expression and current density of key repolarizing currents, prolongation of the APD *in vitro* and *in vivo*, and the reduced expression of intercalated disc proteins. The electrical remodeling of the heart ultimately caused a markedly increased incidence of malignant ventricular arrhythmias and sudden cardiac

death, which occurred prior to the onset of systolic dysfunction, but after the development of cardiomyocyte lipid accumulation. Treating the TG-PPARγ mice, but not WT littermate controls, with a PPARγ agonist increased the incidence of arrhythmias and mortality.

Although PPARγ expression is normally relatively low in the heart, its expression is increased in several forms of heart disease including cardiomyopathy [41], cardiac hypertrophy [42, 43], and in the diabetic heart [44]. Despite its low expression in the heart, tissue-specific loss of PPARγ leads to cardiac hypertrophy with preserved systolic function [17]. PPARγ suppresses cardiac growth and embryonic gene expression and inhibits nuclear-factor κB activity *in vivo* [17] and may also suppress inflammation [45]. The cardiac metabolic abnormalities found in the TG-PPARγ mice, specifically the lipid accumulation within cardiomyocytes [18], mimic many of the abnormalities found in the hearts of diabetic and obese/metabolic syndrome patients [19]. The tissue-restricted TG over-expression of PPARγ enables the preferential shunting of plasma triglycerides and fatty acids to the heart. Pioglitazone-treatment in TG-PPARγ mice would further enhance cardiac PPARγ activity. The systemic effects of pioglitazone in WT mice, in contrast, by channeling a greater proportion of plasma triglycerides and fatty acids to adipose tissues, may actually reduce lipid uptake by the heart relative to the periphery [46]. The differential activation of cardiac vs. peripheral PPARγ, and the shunting and accumulation of lipid in either the heart or the periphery likely account for the TG phenotype and effects of pioglitazone. In WT animals, pioglitazone had no effect on mortality or incidence of ventricular tachyarrhythmias because pioglitazone activation of adipose tissue PPARγ predominates. In the TG-PPARγ mice, although pioglitazone likely activated both cardiac and adipose PPARγ, the level of expression of the cardiac PPARγ likely favored additional cardiomyocyte lipid accumulation and increased electrical remodeling, as reflected by an increased incidence of ventricular tachyarrhythmias, reduced expression of K^+ channels and increased mortality. In humans, the underlying ratio of adipose to cardiac PPARγ expression and the differential effects of different PPARγ agonists – e.g. pioglitazone versus rosiglitazone – likely modulates the beneficial versus toxic effects of these drugs on the heart.

The molecular mechanisms responsible for the reduction in K^+ channel expression in the TG-PPARγ mice are not known. The PPARγ over-expression and lipid loading may exert their effects via transcriptional, translational and/or post-translational processes. Cardiac-specific over-expression of PPARα, a key regulator of diabetes-induced lipid metabolic dysregulation, also induced ion channel remodeling, predominantly a reduction of $I_{to,f}$ and a compensatory increase in I_{ss}[13]. No change in $I_{K,slow}$ current was found in young TG-PPARα mice. In MHC-FATP TG mice, however, the I_{peak} and $I_{K,slow}$ currents were selectively attenuated, without change in $I_{to,f}$ and I_{ss}[14].. In our study of the cardiac-specific overexpression of MHC-PPARγ mice, I_{peak} and $I_{K,slow}$ were significantly reduced, with a trend towards reduction in $I_{to,f}$ current. The remodeling of K^+ channels in the TG-PPARγ mice is similar to the remodeling found in the MHC-FATP mice. In the TG-PPARα and TG-FATP mice, the electrophysiological phenotypes were less severe than the TG-PPARγ mice, and sudden cardiac death (in non-pregnant animals) was not reported [13, 14]. Different transcriptional and/or post-transcriptional pathways may be modified in these mice, which cause changes in distinct K^+ currents. In all three animal models, fatty acid accumulation and utilization are increased. Glucose uptake and metabolism are decreased in the MHC-FATP and MHC-PPARα mice, whereas in the MHC-PPARγ mice, glucose uptake is increased.

Cardiac-specific loss of Cx43 is associated with significant conduction slowing and a higher propensity for the development of ventricular arrhythmias and sudden death [24, 26]. Large reductions of Cx43 expression levels are required to significantly affect epicardial conduction velocities. A 50% reduction of Cx43 protein does not produce significant

conduction slowing, but a 70% to 95% reduction of Cx43 protein results in reduced conduction velocity, increased dispersion of conduction, and enhanced arrhythmogenicity [47-49]. The ~12 week-old TG-PPARγ mice demonstrate ~70% reduction in Cx43 mRNA and ~85% reduction in Cx43 protein amounts. The lack of significant slowing of the conduction velocity in the TG-PPARγ mice suggests that other proteins or post-translational modifications must be compensating for the marked reduction in Cx43 protein levels. Furthermore, the finding of normal conduction velocity implies that the reduction in Cx43 protein in the TG-PPARγ mice does not contribute significantly to the increased incidence of ventricular arrhythmias and mortality. The wide QRS may be due to damage to the His-Purkinje system rather than reduced Cx43 levels. The reduced levels of other intercalated disk proteins is probably not a direct effect of PPARγ since in some cancer models, PPARγ overexpression increases cadherins[50]. The reduction in intercalated disk proteins may contribute to the reduction in Cx43 protein.

In summary, we have found that overexpression of PPARγ in the heart is sufficient to induce action potential remodeling and to cause an acquired long-QT syndrome phenotype. The reduced repolarization reserve increases the incidence of spontaneous ventricular arrhythmias and sudden death. Pioglitazone-treatment increases the incidence of complex ventricular arrhythmias and sudden death in the TG-PPARγ mouse, but not WT littermates. Although an important limitation of this work is that the ion channels responsible for cardiac action potential repolarization in mice are different than in humans, the TG-PPARγ mouse recapitulates an arrhythmic phenotype observed in patients with diabetes and metabolic syndrome.

Supplementary Material

Refer to Web version on PubMed Central for supplementary material.

Acknowledgments

Funding

JPM is supported by the Louis V. Gerstner, Jr. Foundation, Lewis Katz Cardiovascular Research Prize, and NIH K08HL105801. SOM is supported by NIH grants HL068093 and P01 HL081172, the Arlene and Arnold Goldstein Family Foundation, and the Lewis Katz Cardiovascular Research Prize. IJG is supported by NIH grants, HL45095 and HL73029. JD is supported by NIH grant, P01 HL081172. GEM is supported by NIH grant HL076751. CV is supported by NIH grant 1T32HL098129.

References

1. Sharma S, Adrogue JV, Golfman L, Uray I, Lemm J, Youker K, Noon GP, Frazier OH, Taegtmeyer H. Intramyocardial lipid accumulation in the failing human heart resembles the lipotoxic rat heart. FASEB J. 2004; 18:1692–1700. [PubMed: 15522914]
2. Boudina S, Abel ED. Diabetic cardiomyopathy revisited. Circulation. 2007; 115:3213–3223. [PubMed: 17592090]
3. Harmancey R, Wilson CR, Taegtmeyer H. Adaptation and maladaptation of the heart in obesity. Hypertension. 2008; 52:181–187. [PubMed: 18574077]
4. Filippi A, Sessa E Jr. Mazzaglia G, Pecchioli S Jr. Capocchi R Jr. Caprari F, Scivales A, Cricelli C. Out of hospital sudden cardiac death in Italy: a population-based case-control study. J Cardiovasc Med (Hagerstown). 2008; 9:595–600. [PubMed: 18475128]
5. Albert CM, Chae CU, Grodstein F, Rose LM, Rexrode KM, Ruskin JN, Stampfer MJ, Manson JE. Prospective study of sudden cardiac death among women in the United States. Circulation. 2003; 107:2096–2101. [PubMed: 12695299]
6. Balkau B, Jouven X, Ducimetiere P, Eschwege E. Diabetes as a risk factor for sudden death. Lancet. 1999; 354:1968–1969. [PubMed: 10622302]

7. Jouven X, Desnos M, Guerot C, Ducimetiere P. Predicting sudden death in the population: the Paris Prospective Study I. Circulation. 1999; 99:1978–1983. [PubMed: 10209001]
8. Kucharska-Newton AM, Couper DJ, Pankow JS, Prineas RJ, Rea TD, Sotoodehnia N, Chakravarti A, Folsom AR, Siscovick DS, Rosamond WD. Diabetes and the risk of sudden cardiac death, the Atherosclerosis Risk in Communities study. Acta Diabetol. 2009; 47:161–168. [PubMed: 19855920]
9. van Noord C, Sturkenboom MC, Straus SM, Hofman A, Kors JA, Witteman JC, Stricker BH. Serum glucose and insulin are associated with QTc and RR intervals in nondiabetic elderly. Eur J Endocrinol. 2010; 162:241–248. [PubMed: 19897609]
10. Nagaya T, Yoshida H, Takahashi H, Kawai M. Heart rate-corrected QT interval in resting ECG predicts the risk for development of type-2 diabetes mellitus. Eur J Epidemiol. 25:195–202. [PubMed: 20066475]
11. Li W, Bai Y, Sun K, Xue H, Wang Y, Song X, Fan X, Song H, Han Y, Hui R. Patients with metabolic syndrome have prolonged corrected QT interval (QTc). Clin Cardiol. 2009; 32:E93–99. [PubMed: 20014212]
12. Finck BN, Lehman JJ, Leone TC, Welch MJ, Bennett MJ, Kovacs A, Han X, Gross RW, Kozak R, Lopaschuk GD, Kelly DP. The cardiac phenotype induced by PPARalpha overexpression mimics that caused by diabetes mellitus. J Clin Invest. 2002; 109:121–130. [PubMed: 11781357]
13. Marionneau C, Aimond F, Brunet S, Niwa N, Finck B, Kelly DP, Nerbonne JM. PPARalpha-mediated remodeling of repolarizing voltage-gated K+ (Kv) channels in a mouse model of metabolic cardiomyopathy. J Mol Cell Cardiol. 2008; 44:1002–1015. [PubMed: 18482733]
14. Chiu HC, Kovacs A, Blanton RM, Han X, Courtois M, Weinheimer CJ, Yamada KA, Brunet S, Xu H, Nerbonne JM, Welch MJ, Fettig NM, Sharp TL, Sambandam N, Olson KM, Ory DS, Schaffer JE. Transgenic expression of fatty acid transport protein 1 in the heart causes lipotoxic cardiomyopathy. Circ Res. 2005; 96:225–233. [PubMed: 15618539]
15. Marx N, Froehlich J, Siam L, Ittner J, Wierse G, Schmidt A, Scharnagl H, Hombach V, Koenig W. Antidiabetic PPAR gamma-activator rosiglitazone reduces MMP-9 serum levels in type 2 diabetic patients with coronary artery disease. Arterioscler Thromb Vasc Biol. 2003; 23:283–288. [PubMed: 12588772]
16. Zhang L, Chawla A. Role of PPARgamma in macrophage biology and atherosclerosis. Trends Endocrinol Metab. 2004; 15:500–505. [PubMed: 15541649]
17. Duan SZ, Ivashchenko CY, Russell MW, Milstone DS, Mortensen RM. Cardiomyocyte-specific knockout and agonist of peroxisome proliferator-activated receptor-gamma both induce cardiac hypertrophy in mice. Circ Res. 2005; 97:372–379. [PubMed: 16051889]
18. Son NH, Park TS, Yamashita H, Yokoyama M, Huggins LA, Okajima K, Homma S, Szabolcs MJ, Huang LS, Goldberg IJ. Cardiomyocyte expression of PPARgamma leads to cardiac dysfunction in mice. J Clin Invest. 2007; 117:2791–2801. [PubMed: 17823655]
19. Marfella R, Di Filippo C, Portoghese M, Barbieri M, Ferraraccio F, Siniscalchi M, Cacciapuoti F, Rossi F, D'Amico M, Paolisso G. Myocardial lipid accumulation in patients with pressure-overloaded heart and metabolic syndrome. J Lipid Res. 2009; 50:2314–2323. [PubMed: 19470430]
20. Graham DJ, Ouellet-Hellstrom R, MaCurdy TE, Ali F, Sholley C, Worrall C, Kelman JA. Risk of acute myocardial infarction, stroke, heart failure, and death in elderly Medicare patients treated with rosiglitazone or pioglitazone. JAMA. 304:411–418. [PubMed: 20584880]
21. Knollmann BC, Katchman AN, Franz MR. Monophasic action potential recordings from intact mouse heart: validation, regional heterogeneity, and relation to refractoriness. J Cardiovasc Electrophysiol. 2001; 12:1286–1294. [PubMed: 11761418]
22. O'Connell TD, Rodrigo MC, Simpson PC. Isolation and culture of adult mouse cardiac myocytes. Methods Mol Biol. 2007; 357:271–296. [PubMed: 17172694]
23. Hamill OP, Marty A, Neher E, Sakmann B, Sigworth FJ. Improved patch-clamp techniques for high-resolution current recording from cells and cell-free membrane patches. Pflugers Arch. 1981; 391:85–100. [PubMed: 6270629]

24. Danik SB, Liu F, Zhang J, Suk HJ, Morley GE, Fishman GI, Gutstein DE. Modulation of cardiac gap junction expression and arrhythmic susceptibility. Circ Res. 2004; 95:1035–1041. [PubMed: 15499029]
25. Stroud DM, Gaussin V, Burch JB, Yu C, Mishina Y, Schneider MD, Fishman GI, Morley GE. Abnormal conduction and morphology in the atrioventricular node of mice with atrioventricular canal targeted deletion of Alk3/Bmpr1a receptor. Circulation. 2007; 116:2535–2543. [PubMed: 17998461]
26. Gutstein DE, Morley GE, Tamaddon H, Vaidya D, Schneider MD, Chen J, Chien KR, Stuhlmann H, Fishman GI. Conduction slowing and sudden arrhythmic death in mice with cardiac-restricted inactivation of connexin43. Circ Res. 2001; 88:333–339. [PubMed: 11179202]
27. Yang L, Doshi D, Morrow J, Katchman A, Chen X, Marx SO. Protein kinase C isoforms differentially phosphorylate Ca(v)1.2 alpha(1c). Biochemistry. 2009; 48:6674–6683. [PubMed: 19527072]
28. Stypmann J, Engelen MA, Troatz C, Rothenburger M, Eckardt L, Tiemann K. Echocardiographic assessment of global left ventricular function in mice. Lab Anim. 2009; 43:127–137. [PubMed: 19237453]
29. Monnig G, Wiekowski J, Kirchhof P, Stypmann J, Plenz G, Fabritz L, Bruns HJ, Eckardt L, Assmann G, Haverkamp W, Breithardt G, Seedorf U. Phytanic acid accumulation is associated with conduction delay and sudden cardiac death in sterol carrier protein-2/sterol carrier protein-x deficient mice. J Cardiovasc Electrophysiol. 2004; 15:1310–1316. [PubMed: 15574183]
30. Salama G, London B. Mouse models of long QT syndrome. J Physiol. 2007; 578:43–53. [PubMed: 17038432]
31. Hondeghem LM, Carlsson L, Duker G. Instability and triangulation of the action potential predict serious proarrhythmia, but action potential duration prolongation is antiarrhythmic. Circulation. 2001; 103:2004–2013. [PubMed: 11306531]
32. Xu H, Guo W, Nerbonne JM. Four kinetically distinct depolarization-activated K+ currents in adult mouse ventricular myocytes. J Gen Physiol. 1999; 113:661–678. [PubMed: 10228181]
33. Brunet S, Aimond F, Li H, Guo W, Eldstrom J, Fedida D, Yamada KA, Nerbonne JM. Heterogeneous expression of repolarizing, voltage-gated K+ currents in adult mouse ventricles. J Physiol. 2004; 559:103–120. [PubMed: 15194740]
34. London B, Guo W, Pan X, Lee JS, Shusterman V, Rocco CJ, Logothetis DA, Nerbonne JM, Hill JA. Targeted replacement of KV1.5 in the mouse leads to loss of the 4-aminopyridine-sensitive component of I(K,slow) and resistance to drug-induced qt prolongation. Circ Res. 2001; 88:940–946. [PubMed: 11349004]
35. Xu H, Barry DM, Li H, Brunet S, Guo W, Nerbonne JM. Attenuation of the slow component of delayed rectification, action potential prolongation, and triggered activity in mice expressing a dominant-negative Kv2 alpha subunit. Circ Res. 1999; 85:623–633. [PubMed: 10506487]
36. Guo W, Xu H, London B, Nerbonne JM. Molecular basis of transient outward K+ current diversity in mouse ventricular myocytes. J Physiol. 1999; 521:587–599. [PubMed: 10601491]
37. Niwa N, Wang W, Sha Q, Marionneau C, Nerbonne JM. Kv4.3 is not required for the generation of functional Ito,f channels in adult mouse ventricles. J Mol Cell Cardiol. 2008; 44:95–104. [PubMed: 18045613]
38. Paolisso G, Gualdiero P, Manzella D, Rizzo MR, Tagliamonte MR, Gambardella A, Verza M, Gentile S, Varricchio M, D'Onofrio F. Association of fasting plasma free fatty acid concentration and frequency of ventricular premature complexes in nonischemic noninsulin- dependent diabetic patients. Am J Cardiol. 1997; 80:932–937. [PubMed: 9382011]
39. Pietrasik G, Goldenberg I, McNitt S, Moss AJ, Zareba W. Obesity as a risk factor for sustained ventricular tachyarrhythmias in MADIT II patients. J Cardiovasc Electrophysiol. 2007; 18:181–184. [PubMed: 17338766]
40. Szczepaniak LS, Victor RG, Orci L, Unger RH. Forgotten but not gone: the rediscovery of fatty heart, the most common unrecognized disease in America. Circ Res. 2007; 101:759–767. [PubMed: 17932333]

41. Harris GS, Lust RM, DeAntonio JH, Katwa LC. PPAR-gamma expression in animals subjected to volume overload and chronic Urotensin II administration. Peptides. 2008; 29:795–800. [PubMed: 18423937]

42. Gomez-Garre D, Herraiz M, Gonzalez-Rubio ML, Bernal R, Aragoncillo P, Carbonell A, Rufilanchas JJ, Fernandez-Cruz A. Activation of peroxisome proliferator-activated receptor-alpha and -gamma in auricular tissue from heart failure patients. Eur J Heart Fail. 2006; 8:154–161. [PubMed: 16185925]

43. Krishnan J, Suter M, Windak R, Krebs T, Felley A, Montessuit C, Tokarska-Schlattner M, Aasum E, Bogdanova A, Perriard E, Perriard JC, Larsen T, Pedrazzini T, Krek W. Activation of a HIF1alpha-PPARgamma axis underlies the integration of glycolytic and lipid anabolic pathways in pathologic cardiac hypertrophy. Cell Metab. 2009; 9:512–524. [PubMed: 19490906]

44. Lee TI, Kao YH, Chen YC, Pan NH, Chen YJ. Oxidative stress and inflammation modulate peroxisome proliferator-activated receptors with regional discrepancy in diabetic heart. Eur J Clin Invest. 2010; 40:692–699. [PubMed: 20561028]

45. Pascual G, Sullivan AL, Ogawa S, Gamliel A, Perissi V, Rosenfeld MG, Glass CK. Anti-inflammatory and antidiabetic roles of PPARgamma. Novartis Found Symp. 2007; 286:183–196. [PubMed: 18269183]

46. Vikramadithyan RK, Hirata K, Yagyu H, Hu Y, Augustus A, Homma S, Goldberg IJ. Peroxisome proliferator-activated receptor agonists modulate heart function in transgenic mice with lipotoxic cardiomyopathy. J Pharmacol Exp Ther. 2005; 313:586–593. [PubMed: 15671204]

47. Morley GE, Vaidya D, Samie FH, Lo C, Delmar M, Jalife J. Characterization of conduction in the ventricles of normal and heterozygous Cx43 knockout mice using optical mapping. J Cardiovasc Electrophysiol. 1999; 10:1361–1375. [PubMed: 10515561]

48. Danik SB, Rosner G, Lader J, Gutstein DE, Fishman GI, Morley GE. Electrical remodeling contributes to complex tachyarrhythmias in connexin43-deficient mouse hearts. FASEB J. 2008; 22:1204–1212. [PubMed: 17984180]

49. van Rijen HV, Eckardt D, Degen J, Theis M, Ott T, Willecke K, Jongsma HJ, Opthof T, de Bakker JM. Slow conduction and enhanced anisotropy increase the propensity for ventricular tachyarrhythmias in adult mice with induced deletion of connexin43. Circulation. 2004; 109:1048–1055. [PubMed: 14967725]

50. Lee HJ, Su Y, Yin PH, Lee HC, Chi CW. PPAR(gamma)/PGC-1(alpha) pathway in E-cadherin expression and motility of HepG2 cells. Anticancer Res. 2009; 29:5057–5063. [PubMed: 20044617]

CLINICAL PERSPECTIVE

Diabetes and obesity confer an increased risk of sudden cardiac death and are associated with cardiomyocyte lipid accumulation and altered cardiac electrical properties (demonstrated by prolongation of the QRS and QT intervals). In order to study the effects of metabolic abnormalities on arrhythmias without the complex systemic effects of diabetes and obesity, we studied a mouse model with cardiac-specific overexpression of PPARγ, a transcription factor that is a key regulator of glucose and lipid metabolism. These PPARγ-transgenic mice develop abnormal accumulation of intracellular lipids and die as young adults, prior to a significant reduction in systolic function. We found that these mice have prolongation of the QT interval, and spontaneous ventricular arrhythmias, including polymorphic ventricular tachycardia and ventricular fibrillation. Isolated cardiomyocytes demonstrated prolonged action potential duration caused by reduced potassium currents, which are responsible for repolarization. Short-term exposure to pioglitazone, a PPARγ agonist, had no effect on mortality or rhythm in WT mice, but further exacerbated the arrhythmic phenotype and increased the mortality in the PPARγ mice. Our findings support an important link between PPARγ activation, cardiomyocyte lipid accumulation, ion channel remodeling and increased cardiac mortality. This mouse model may help identify the molecular mechanisms leading to sudden death in diabetic and/or obese patients

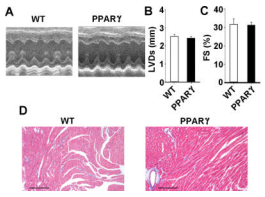

Figure 1.

Normal cardiac function in 10-12 week old PPARγ mice. A, Representative M-mode echocardiographic images from a wild-type (WT) littermate control and PPARγ mice. B and C, Graphs of left ventricular systolic diameter (LVDs) and fractional shortening. The values are presented as mean + SEM; (n= 6 for WT and 11 for PPARγ). D, Representative Masson's trichrome stain of ventricular tissue from WT littermate and PPARγ mice. Collagen appears as a light blue stain. Scale bars: 70 μm.

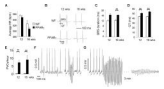

Figure 2.

Electrocardiograms of PPARγ mice. A, Average daily heart rate of 12 week and 16 week old mice, 3 animals in each group. Mean + SEM. B, Representative ECGs of PPARγ mice and WT littermates. QRS and QT intervals are indicated by brackets. C-D, Graphs of QRS duration and QT interval from WT and PPARγ mice. The values are presented as mean + SEM. ** $p<0.025$ by U-test. E, Graph of PVCs per hour, recorded in unrestrained mice. The values are presented as mean + SEM. n= 4 or 5 mice per group. ** $p<0.025$ by U-test. F, Representative telemetry recordings of PPARγ mice showing frequent PVCs (left) and non-sustained ventricular tachycardia (right). G, Fatal ventricular tachycardia followed by an agonal rhythm in a PPARγ mouse.

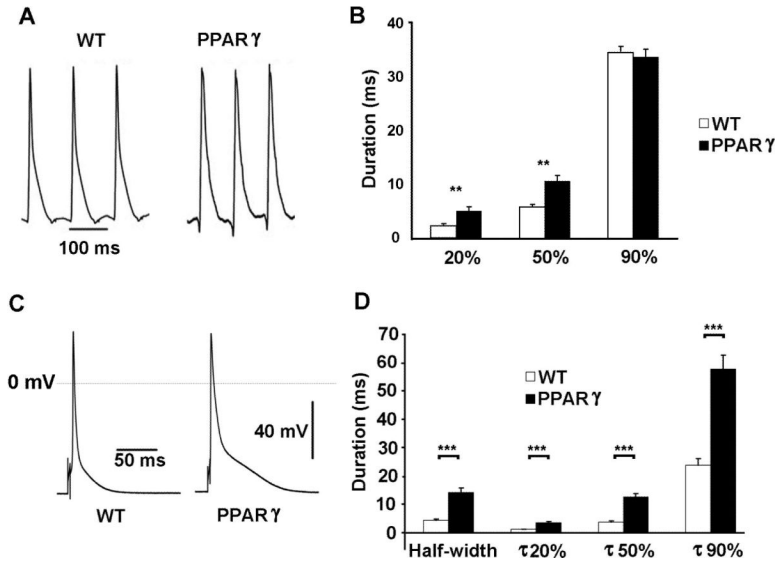

Figure 3.

Action potential waveforms in WT and PPARγ mice. A, Representative *in vivo* monophasic action potential recordings from WT and PPARγ mice, mean RR interval 117 ms and 113 ms respectively. B, Graph of MAP recordings at 20%, 50% and 90% repolarization. WT: n=6; PPARγ: n=5. Mean ± SEM; **=p<0.01. C, Representative cardiomyocyte action potential waveforms from WT and PPARγ mice. D, Graph of APD at half-width, 20%, 50% and 90% repolarization. WT: n=24; PPARγ: n=39. Mean ± SEM; *** p<0.001.

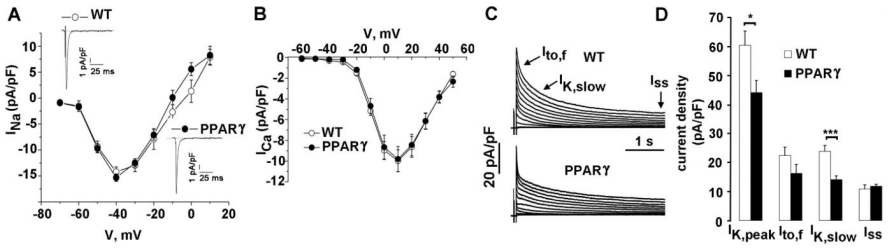

Figure 4.

Properties of Na^+, Ca^{2+} and K^+ currents. A, I-V relationship for Na^+ current in WT and PPARγ mice. Insets: WT and PPARγ current traces. B, I-V relationship for Ca^{2+} current. C, Voltage-dependent K^+ current tracings for WT and PPARγ mice. Cardiomyocytes were held at a holding potential of -80 mV. A brief (15 ms) voltage step to -40 mV was used to activate and inactivate Na^+ channels. Following a brief return to -80 mV, voltage-dependent K^+ currents were elicited with voltage steps between -60 mV and +50 mV in 10 mV-increment, for 4 sec with 10 sec interval. D, Graph of current density of $I_{K,\,peak}$, $I_{to,f}$, $I_{K,slow}$ and I_{ss} currents. The decay phases of the outward K^+ currents evoked during 4.0 sec depolarizing voltage step to +40 mV were fit by a double exponential function. Mean + SEM. WT: n=43; PPARγ: n=31. * =p <0.05, *** =p <0.001

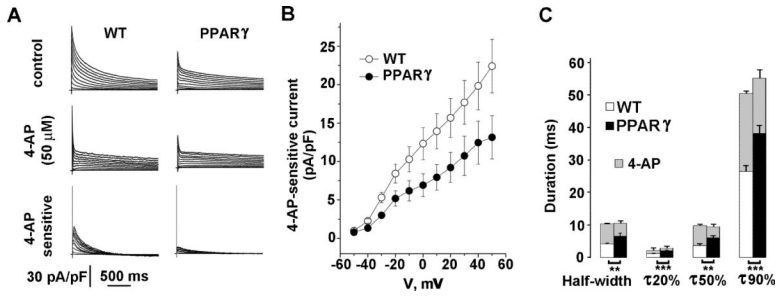

Figure 5.

Reduced $I_{K,slow}$ is responsible for APD prolongation in TG-PPARγ mice. A, Representative voltage-dependent K^+ current tracings from WT and PPARγ mice (top), after exposure to 50 μM 4-AP (middle) and the 4-AP sensitive current (bottom). Patch clamp protocols are described in Methods and Figure 4. 4-AP sensitive current was obtained by off-line digital subtraction of records before and after 4-AP application. B, Graph of current density of 4-AP sensitive current for WT and TG-PPARγ mice. WT: n=26; PPARγ: n=21. Mean ± SEM. C, Graph of APD before and after (grey) 4-AP exposure. Prior to 4-AP exposure, differences at half-width, 20%, 50% and 90% repolarization between WT and PPARγ are statistically significant (** $p<0.01$, *** $p<0.001$). After 4-AP (grey bars), differences between WT and PPARγ are not statistically significant. WT: n=34; PPARγ: n=22. Mean + SEM.

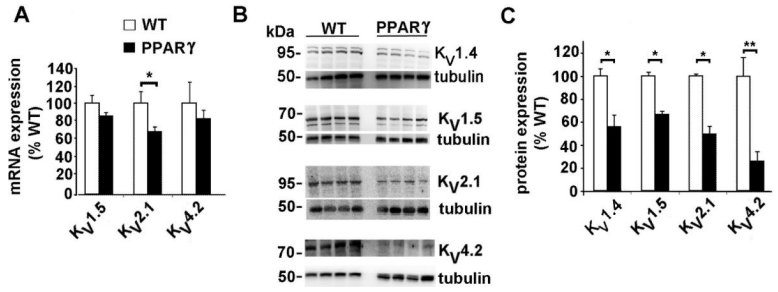

Figure 6.

mRNA and protein expression of K^+ channels. A, mRNA expression, measured by real-time qPCR of K^+ channel pore-forming α subunits of $I_{K,slow}$ and $I_{to,f}$. n= 4 or 5 animals in each group. * $p<0.05$ by U-test. B, Immunoblots of K^+ channels with tubulin loading controls. C, Bar graph of protein expression of indicated K^+ channel subunits in PPARγ mice (black bars) relative to WT littermate mice (white bars). Mean image intensity in arbitrary units (measured using ImageJ) was normalized to tubulin signal and expressed as percent of WT control mice. Mean + SEM. * $p<0.05$; ** $p<0.01$ by U-test

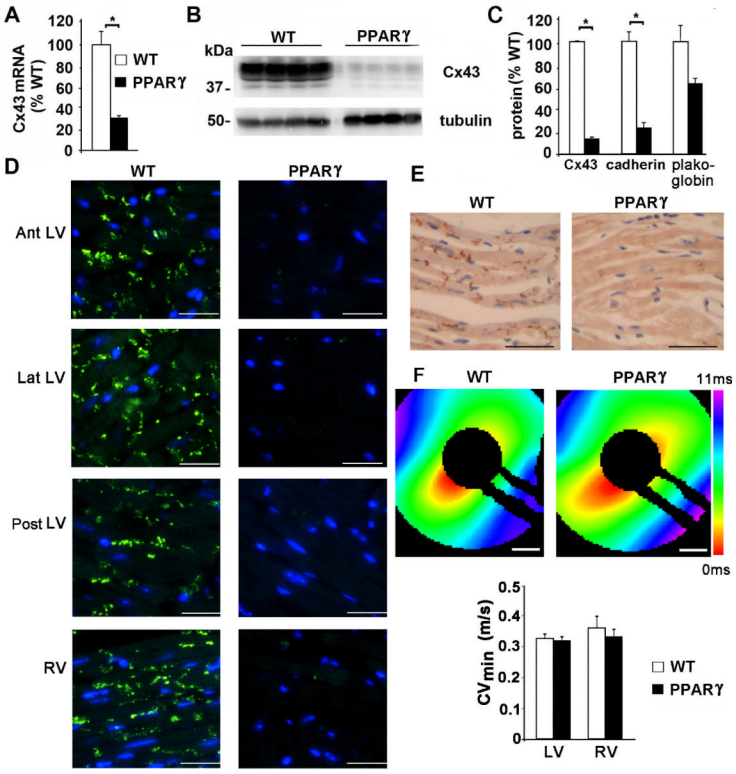

Figure 7.

Reduced Cx43 mRNA and protein expression in PPARγ mice. A, mRNA expression of Cx43, normalized to WT. n= 4 mice in each group. * $p<0.05$ by U-test. B, Immunoblot of Cx43 (with tubulin as a loading control) from mouse ventricular tissue, n=4 mice in each group. * $p<0.05$ by U-test. C, Graph of Cx43 expression in PPARγ mice, normalized to WT littermate control. D, Immunofluorescence of Cx43 protein (bright green) from indicated ventricular tissue. Scale bar: 75 μm. E, DAB staining for Cx43 (dark brown) from WT littermate and PPARγ mice. Scale bar: 45 μm. F, Representative activation maps showing conduction across the ventricular epicardium of control and TG-PPARγ mice. Scale bar: 1 mm. Lower, bar graph of LV and RV CV_{min} for WT and PPARγ mice.

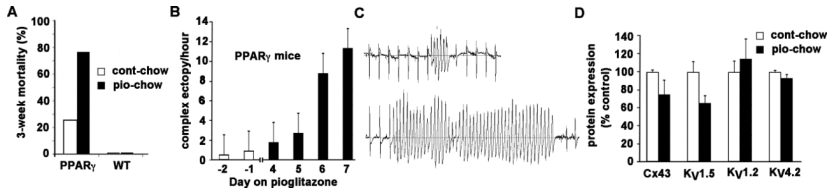

Figure 8.

Pioglitazone increases mortality and ventricular arrhythmias in TG-PPARγ, but not WT mice. A, Bar graph of 3-week mortality of TG-PPARγ and WT mice fed either control-chow or pioglitazone-chow. n=8 in each group. B, Bar graph of average complex ventricular ectopy per hour in the PPARγ mice fed control (white bars) and pioglitazone-chow (black bars). Error bars are SEM. n=4 mice. C, Representative telemetry recordings of TG-PPARγ mice fed pioglitazone showing non-sustained ventricular tachycardia. D, Bar graph of protein expression of Cx43 and K^+ channel subunits in TG-PPARγ mice fed pioglitazone (black bars) relative to TG-PPARγ mice fed control chow (white bars). Mean image intensity was normalized to tubulin signal and expressed as percent of control-chow fed TG-PPARγ. Mean + SEM, n=4 animals in each group.